Solution and Solvent-Free Stopper Exchange Reactions for the Preparation of Pillar[5]arene-containing [2] and [3]Rotaxanes

Nihed Becharguia, Iwona Nierengarten, Jean-marc Strub, Sarah Cianférani, Marine Rémy, Emeric Wasielewski, Rym Abidi, Jean-Francois Nierengarten

Chemistry–A European Journal
Research Article
doi.org/10.1002/chem.202304131
Chemistry Europe
European Chemical Societies Publishing
www.chemeurj.org

Solution and Solvent-Free Stopper Exchange Reactions for the Preparation of Pillar[5]arene-containing [2] and [3]Rotaxanes

Nihed Becharguia,[a, b] Iwona Nierengarten,*[a] Jean-Marc Strub,[c] Sarah Cianférani,[c] Marine Rémy,[a] Emeric Wasielewski,[d] Rym Abidi,[b] and Jean-François Nierengarten*[a]

Dedicated to Prof. Yves Rubin on the occasion of his 60th birthday

Diamine reagents have been used to functionalize a [2]rotaxane building block bearing an activated pentafluorophenyl ester stopper. Upon a first acylation, an intermediate host-guest complex with a terminal amine function is obtained. Dissociation of the intermediate occurs in solution and acylation of the released axle generates a [2]rotaxane with an elongated axle subunit. In contrast, the corresponding [3]rotaxane can be obtained if the reaction conditions are appropriate to stabilize the inclusion complex of the mono-amine intermediate and the pillar[5]arene. This is the case when the stopper exchange is performed under mechanochemical solvent-free conditions. Alternatively, if the newly introduced terminal amide group is large enough to prevent the dissociation, the second acylation provides exclusively a [3]rotaxane. On the other hand, detailed conformational analysis has been also carried out by variable temperature NMR investigations. A complete understanding of the shuttling motions of the pillar[5]arene subunit along the axles of the rotaxanes reported therein has been achieved with the help of density functional theory calculations.

Introduction

Interlocked molecular ensembles such as rotaxanes and catenanes are fascinating systems in which large amplitude molecular motions are possible.[1] Chemists became rapidly interested in controlling the conformation of such molecules and the pioneering work of Sauvage and Stoddart in this area gave rise to the field of molecular machines.[2] The possible applications of such systems in various fields including biology,[3] nanotechnology[4] or catalysis[5] have been a strong driving force to further improve the synthetic strategies allowing to efficiently produce mechanically interlocked molecules.[6] Their preparation remains often challenging as pre-organization of separate molecular units into a well-defined supramolecular structure is mandatory. For example, the most classical approach to prepare rotaxanes is based on the grafting of bulky stoppers onto a linear building block associated to a macrocyclic moiety in an inclusion complex.[7] This strategy is efficient as long as the reaction conditions are compatible with the formation of the supramolecular complex. This requirement is however often problematic, in particular when weak intermolecular interactions are used to assemble the two components. This is for example the case when pillar[5]arene is used as the macrocyclic component for the preparation of rotaxanes.[8–10] The direct preparation of rotaxanes from pillar[5]arene-based inclusion complexes is highly dependent on the nature of the reagents even when similar reactions are used for their synthesis and yields are often quite moderate.[9,10] To solve this problem, we have developed the preparation of pillar[5]arene-containing [2]rotaxane building blocks allowing their efficient post-modification by a stopper exchange reaction.[11–13] Very recently, we have also shown that the reactivity of symmetrical pillar[5]arene-based building block is affected by the presence of the macrocyclic subunit.[14] Indeed, the first stopper exchange reaction is fast while the second always significantly slower thus allowing selective mono-

[a] Dr. N. Becharguia, Dr. I. Nierengarten, Dr. M. Rémy, Dr. J.-F. Nierengarten
Laboratoire de Chimie des Matériaux Moléculaires
Université de Strasbourg et CNRS (UMR 7042, LIMA), Ecole Européenne de Chimie, Polymères et Matériaux
25 rue Becquerel, 67087 Strasbourg Cedex 2, France
E-mail: iosinska@unistra.fr
nierengarten@unistra.fr
Homepage: http://nierengartengroup.com
[b] Dr. N. Becharguia, Prof. R. Abidi
Laboratoire d'Applications de la Chimie aux Ressources et Substances Naturelles et l'Environnement
Faculté des Sciences de Bizerte, Université de Carthage
7021 Zarzouna Bizerte, Tunisia
[c] Dr. J.-M. Strub, Dr. S. Cianférani
Laboratoire de Spectrométrie de Masse BioOrganique
Université de Strasbourg et CNRS (UMR 7178, IPHC), Ecole Européenne de Chimie, Polymères et Matériaux
25 rue Becquerel, 67087 Strasbourg Cedex 2, France
[d] Dr. E. Wasielewski
Plateforme RMN Cronenbourg
Université de Strasbourg et CNRS (UMR 7042, LIMA)
Ecole Européenne de Chimie, Polymères et Matériaux
25 rue Becquerel, 67087 Strasbourg Cedex 2, France

Supporting information for this article is available on the WWW under https://doi.org/10.1002/chem.202304131

functionalization of the rotaxane building block in high yields. By using this methodology, rotaxane building block **2** is easily available on a multigram scale (Figure 1).

In this paper, we show that mono-functionalized building block **2** can be used for the direct synthesis of [2]rotaxanes with elongated axle moieties and [3]rotaxanes. For this purpose, diamine reagents have been used to functionalize building block **2**. As schematically shown in Figure 2, a first acylation of diamine reagent **3** with [2]rotaxane **2** generates an intermediate

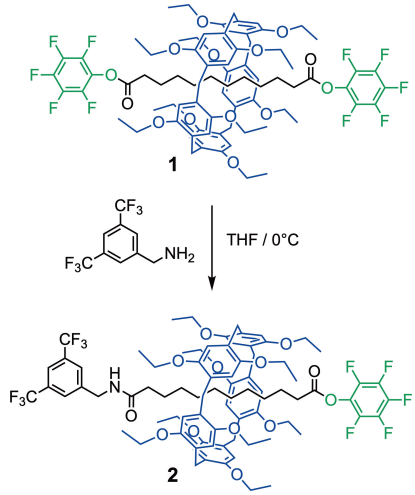

Figure 1. Owing to a protecting effect resulting from the presence of the macrocyclic moiety, mono-functionalization of **1** with an amine reagent is very efficient, compound **2** is thus obtained in 97% yield by reaction of **1** with 3,5-bis(trifluoromethyl)benzylamine.[14]

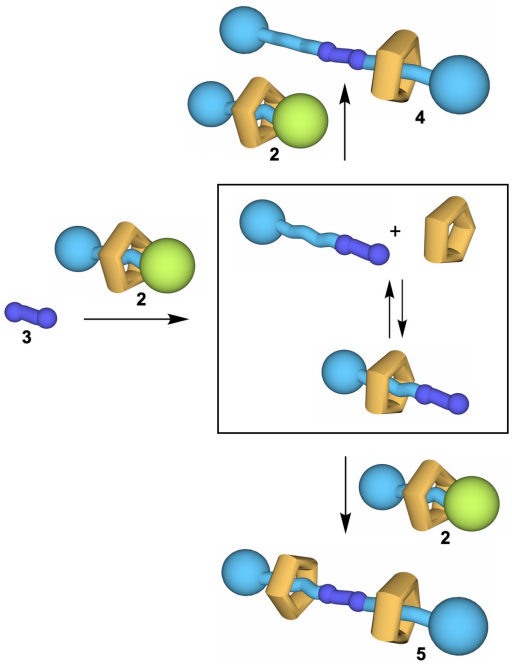

Figure 2. Schematic representation of the reaction of a diamine reagent (**3**) with [2]rotaxane building block **2** incorporating a pentafluorophenyl ester stopper (in green). The outcome depends on the stability of the intermediate host-guest complex and is either a [2]rotaxane with an elongated axle (**4**) or a [3]rotaxane (**5**).

[2]rotaxane with a terminal amine function. The outcome of the reaction is then related on the ability of the pillar[5]arene to escape from its axle. If the newly introduced terminal amide group is large enough to prevent the dissociation of the intermediate, the second acylation provides a [3]rotaxane (**5**). In contrast, if dissociation is possible, the reaction of the uncomplexed axle intermediate with a second equivalent of **2** generates a [2]rotaxane with an elongated axle subunit (**4**). On the other hand, the corresponding [3]rotaxane can be obtained if the reaction conditions are appropriate to stabilize the inclusion complex of the mono-amine intermediate and the pillar[5]arene. This is effectively the case when the stopper exchange is performed under solvent-free conditions.

Results and Discussion

Stopper exchange with diamine reagents in solution

Building block **2** was treated with diamines **3a–d** (0.5 equiv.) to form the corresponding [2]rotaxanes (**4a–d**) with an elongated axle moiety (Scheme 1). In all the cases, a first stopper exchange reaction occurred to generate an intermediate host-guest complex from which the pillar[5]arene unit was liberated thus providing an intermediate axle with a terminal amine function. Subsequent reaction of this intermediate with a second equivalent of **2** then provided [2]rotaxanes **4a–d**. No traces of [3]rotaxanes could be detected thus showing that dissociation of the intermediate host-guest complexes was always faster than the second stopper exchange reaction. In contrast, when the reaction of **2** was carried out with amine **3e**, [3]rotaxane **5e** was exclusively obtained as the disubstituted naphthalene moiety is large enough to prevent dissociation of the intermediate obtained after reaction of **2** with **3e**. In other words, the intermediate is a [2]rotaxane in this particular case. It can be noted that compound **5e** was obtained as a 1:1 mixture of two diastereomers depending on the relative stereochemistry of the two pillar[5]arene moieties (Figure S1). The two macrocycles of the [3]rotaxane have an opposite absolute stereochemistry in the case of the achiral *meso* diastereomer. In contrast, the absolute chemistry of the two pillar[5]arenes is the same in the case of the C_2-symmetrical diastereomer. The C_s- and C_2-symmetrical diastereomers of **5e** have an identical polarity and could not be separated.

Stopper exchange with diamine reagents under solvent-free ball-milling conditions

Mechanochemical solvent-free conditions have been successfully used to prepare rotaxanes.[15–17] Our group has shown that such conditions are particularly well suited to obtain pillar[5]arene-containing rotaxanes in good yields.[16] Indeed, the association between the axle reagent and the pillar[5]arene leading to rotaxane formation is favored in the solid state.[17] When compared to analogous reactions performed in solution, desolvation energy is totally removed in the solid state.

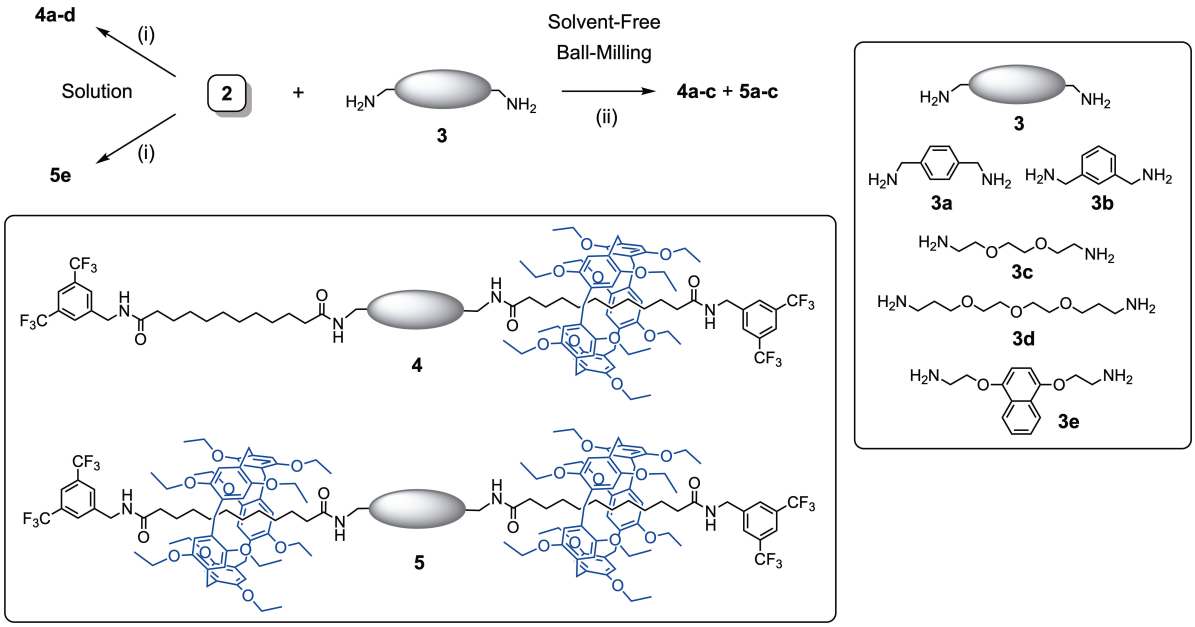

Scheme 1. Reaction of [2]rotaxane **2** with various diamines. *Reagents and conditions*: (i) THF, rt (**4a**: 94% from **3a**; **4b**: 89% from **3b**; **4c**: 93%from **3c**; **4d**: 95% from **3d**; **5e**: 99% from **3e**); (ii) TBD (2 equiv.), mixing in a Retsch MM400 mill at 30 Hz for 2 h [**4a**: 50% and **5a**: 47% (from **3a**); **4b**: 29% and **5b**: 68% (from **3b**); **4c**: 72% and **5c**: 24% (from **3c**)].

Moreover, the concentration effect is also favorable to generate the inclusion complex in the solid state. Our group has also reported solvent-free conditions for stopper exchange reactions involving pillar[5]arene-containing rotaxane building blocks with pentafluorophenyl ester stoppers and various nucleophiles.[11c] Under such conditions, one may anticipate that the reaction of **2** with diamine reagents **3a–c** should allow the formation of the corresponding [3]rotaxanes as dissociation of the intermediate host-guest complexes should be limited in the solid state. The mechanochemical solvent-free conditions for the stopper exchange reaction were first optimized with diamine **3a** (Scheme 1, Table 1).

The stopper exchange reaction was very slow by mixing diamine **3a** with a slight excess of rotaxane building block **2** in a Retsch MM400 mill at 30 Hz for 2 hours (Table 1, Entry 1). In this case, acylated products were obtained in low yields together with large amounts of unreacted starting materials. Whereas good yields are typically obtained when using stoichiometric amounts of pentafluorophenyl esters and amine reagents in THF solutions, it has been shown that the use of a large excess of amine reagents (8 equiv.) is mandatory to achieve such reactions in good yields under mechanochemical conditions.[11c] It was however not possible to use an excess of diamine reagent **3a** for the functionalization of **2** as such conditions would produce large amounts of mono-acetylated byproducts. It was therefore decided to add a base to the mixture. Mixing of **3a** and **2** was thus carried out in the presence of 1,5,7-triazabicyclo[4.4.0.]dec-5-ene (TBD). The starting materials were not totally consumed after 2 hours when 1 equiv. of TBD was used (Table 1, Entry 2), the reaction was nevertheless much faster than in the absence of additive. By increasing the amount of TBD to 2 equiv. (Entry 3), the starting materials were fully consumed after two hours of mixing. Whereas the reaction of **3a** and **2** in THF solutions provided exclusively [2]rotaxane **4a**, mechanochemical conditions afforded a mixture of [2] and [3]rotaxanes thus showing that dissociation of the intermediate host-guest complex is significantly prevented in the solid state. Compounds **4a** and **5a** were then conveniently separated by size exclusion chromatography. The isolated yields in **4a** and **5a** were 50 and 47%, respectively. By further increasing the amount of TBD (4 equiv.), the overall yield was similar but the formation of [3]rotaxane **5a** was slightly less favorable (Entry 4, Table 1). This observation can be explained by a dilution effect that favors dissociation of the pseudorotaxane intermediate to a greater extend. Alternatively, it was also possible to use 4-dimethylaminopyridine

Table 1. Optimization of the mechanochemical solvent-free conditions for the reaction of **2** (2.2 equiv.) with diamine **3a** (1 equiv.). All the reactions were performed in a 10 mL stainless-steel vial containing four stainless-steel balls that was mixed in a Retsch MM400 mill at 30 Hz for 2 h.

Entry	Additive	Isolated yield in [2]rotaxane **4a**	Isolated yield in [3]rotaxane **5a**
1	None	9%	8%
2	TBD (1 equiv.)	51%	17%
3	TBD (2 equv.)	50%	47%
4	TBD (4 equv.)	55%	41%
5	DMAP (2 equiv.)	46%	37%

(DMAP) as a base, but the overall yield was not as good as the one obtained with TBD (Entry 5, Table 1).

The mechanochemical reaction conditions optimized with diamine **3a** were then used starting from **3b**–**c** (Scheme 1). A mixture of the appropriate diamine reagent (1 equiv.), **2** (2.2 equiv.) and TBD (2 equiv.) was mixed in a Retsch MM400 mill at 30 Hz for 2 hours. The resulting solid was dissolved in $CHCl_3$ and filtered over a short plug of silica. [2]Rotaxane **4a**–**c** and [3]rotaxane **5a**–**c** were then separated by gel permeation chromatography (Biobeads SX-1, $CHCl_3$). The overall yield in rotaxane was the same whatever the diamine reagent (96-97%), however the relative proportion of [2] and [3]rotaxane was significantly affected by the nature of the linker between the two amine functions of **3a**–**c**. Diamine reagents **3a**–**b** with phenylene spacers gave effectively higher yields in [3]rotaxane when compared to triethylene glycol diamine (**3c**). Structural factors play obviously an important role on the stability of the intermediate pseudorotaxane obtained after the first acylation. The nature of the spacer may influence the dissociation kinetics. The energy barrier required for the unthreading process actually depends on the size of the spacer. This effect is consistent with the better yields in [3]rotaxane obtained from **3b**, the dethreading of the pillar[5]arene macrocycle through the *meta*-phenylene linker being significantly more difficult (*vide supra*). On the other hand, the system maybe dynamic and association/dissociation of the pseudorotaxane intermediate is in principle possible during the reaction.[17] Owing to the very poor affinity of oligoethylene glycol for the pillar[5]arene, the threading process of the axle component terminated with the ethylene glycol amine is likely not very favorable.

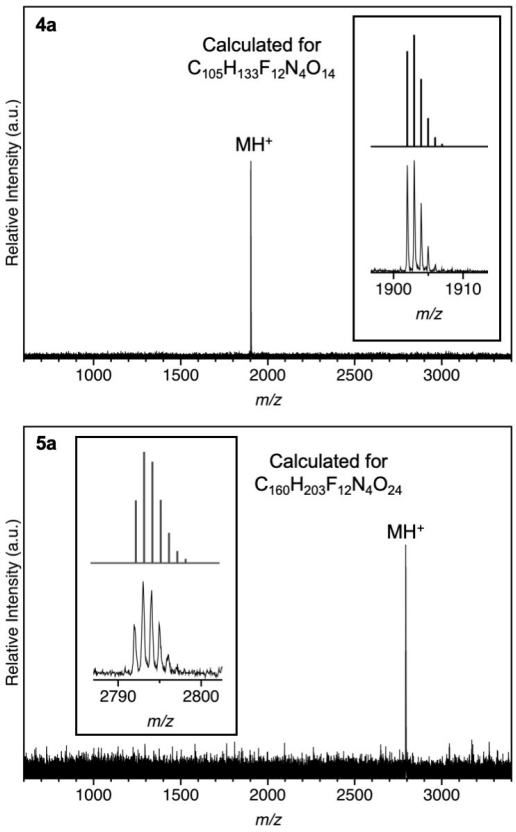

Figure 3. MALDI-TOF mass spectra of compounds **4a** and **5a** recorded in the positive mode. Inset: calculated (top) and experimental (bottom) isotopic patterns

Characterization of the rotaxanes

Compounds **4a**–**d**, **5a**–**c** and **5e** were characterized by a combination of different analytical techniques. Matrix-assisted laser desorption – time of flight (MALDI-TOF) mass spectrometry confirmed the proposed structures of **4a**–**d**, **5a**–**c** and **5e**. As typical examples, the mass spectra recorded for compounds **4a** and **5a** in the positive mode are depicted in Figure 3. In all the cases, only the singly charged pseudo-molecular ion peak corresponding to $[M+H]^+$ was observed. Under these experimental conditions, no fragmentation occurred thus showing that MALDI-TOF mass spectrometry is an ideal tool for the characterization of such rotaxanes.

[3]Rotaxanes **5a**–**c** and **5e** were also characterized by NMR spectroscopy. As a typical example, the ^{1}H NMR spectra recorded for [3]rotaxane **5a** in $CDCl_3$ and DMSO-d_6 are depicted in Figure 4. Considering the shielding effect of the pillar[5]arene moiety on the resonances of the methylene groups located within its cavity, each macrocycle is clearly located over a decyl subunit of the axle. All the signals of the CH_2 units of the decyl chain are affected by the ring current effect of the aromatic ring of their pillar[5]arene component thus showing that gliding motions of the pillar[5]arenes all over their decyl station are faster than the NMR timescale under these conditions. In $CDCl_3$, the shielding is more important for H(3,4) showing that these particular methylene groups have a higher probability of presence into the cavity of the macrocycle. As already shown with related [2]rotaxanes,[14] intramolecular dipole-dipole interactions play a major role in nonpolar solvents and conformations in which the macrocycle is close to its bis(trifluoromethyl)phenyl stoppers are favored. When going from $CDCl_3$ to DMSO-d_6, dramatic chemical shift changes are observed for the resonances of the methylene groups of the decyl chains. Analysis of the relative chemical shifts of the methylene groups revealed that the pillar[5]arene moiety is preferentially located in the middle of the decyl chains in DMSO. Under these conditions, the conformational preferences of rotaxane **5a** result from solvophobic effects. Obviously, the amide functions of **5a** are well solvated by DMSO while repulsive interactions between the decyl chain and the polar solvent molecules are expected. As a result, the macrocycle is preferentially located in the middle of the axle subunit to limit unfavorable interactions between the decyl chain and the solvent. A similar behavior was also observed for [3]rotaxanes **5b**, **5c** and **5e** (Figure S2). Finally, it should be added that compounds **5a**–**c** and **5e** were all obtained as a 1:1 mixture of two diastereomers. However, the NMR spectra of the two diastereomers recorded at room temperature are identical in all the cases. Actually, it was necessary to record the spectra at low temperature to distinguish the two diastereomers (Figure S3). At room temperature, dynamic exchanges are fast and thermal agitation

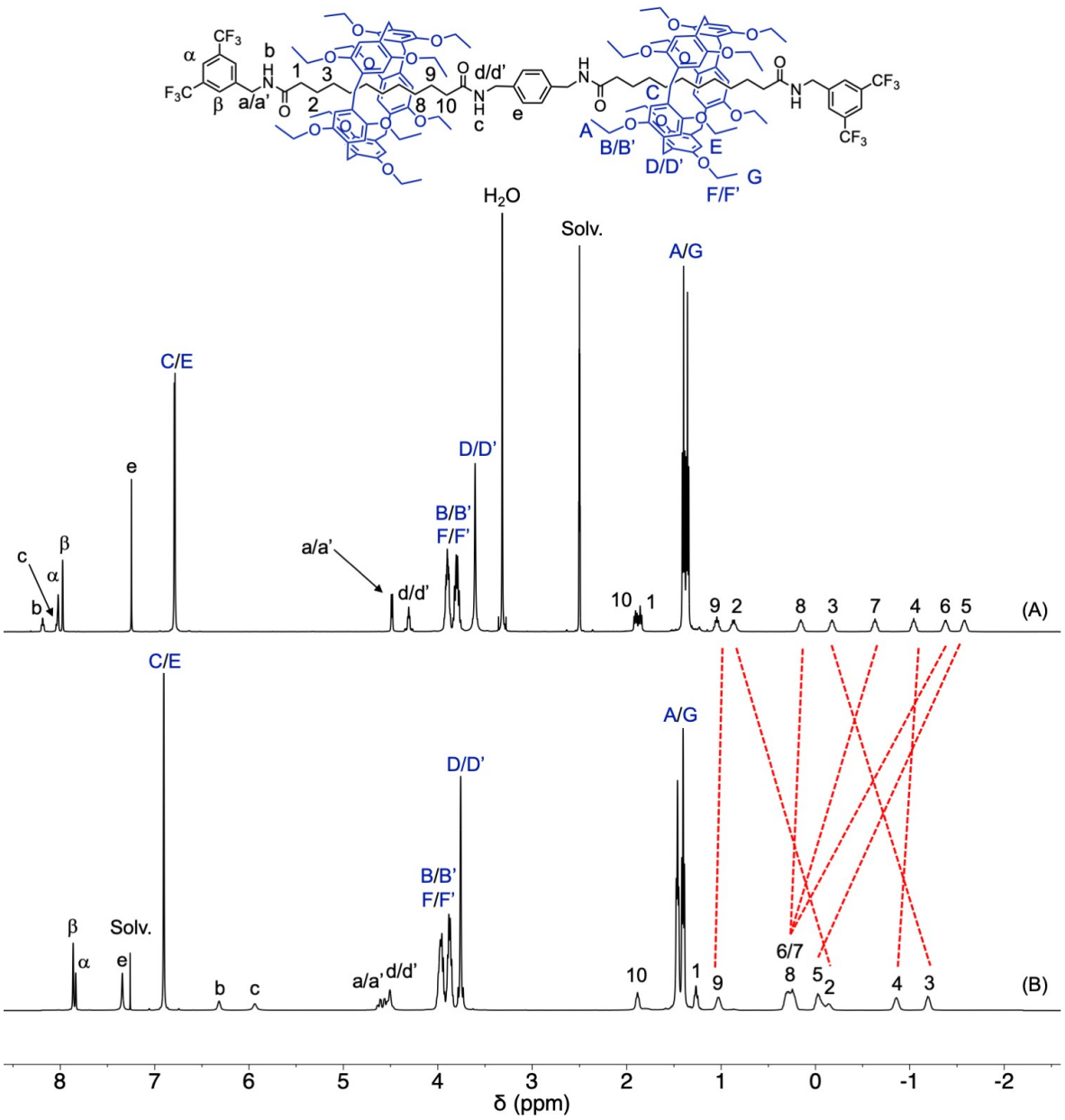

Figure 4. ^{1}H NMR spectra (500 MHz, 298 K) recorded for [3]rotaxane **5a** in DMSO-d_6 (A) and $CDCl_3$ (B).

prevents the transfer of the chiral information.[18] By lowering the temperature, molecular motions are in principle more limited. The ^{1}H NMR spectrum recorded at 208 K for **5e** revealed effectively clearly the presence of the two diastereomers. In contrast, only minor differences were observed in the ^{1}H NMR spectra recorded at low temperature for **5a**–**c**.

Compounds **4a**–**d** were also characterized by NMR spectroscopy. As shown in Figure 5, the ^{1}H NMR spectrum of **4a** recorded in $CDCl_3$ at room temperature revealed that the two 3,5-bis(trifluoromethyl)benzyl stoppers appear as equivalent suggesting fast dynamic gliding motions of the pillar[5]arene moiety along the molecular axle of the rotaxane. The dynamic shuttling must be however close to the NMR timescale under these conditions as the signals arising from the two decyl chains are broad (Figure S4). This prompted us to perform temperature-dependent NMR measurements. At low temperature, the dynamic gliding motions became slower than the NMR timescale and the two moieties of the axle of **4a** appeared as non-equivalent in the ^{1}H NMR spectrum recorded at 218 K in $CDCl_3$ (Figure 5).

Considering the dramatic shielding effect of the pillar[5]arene moiety on the resonances of the groups located within its cavity, it appears clear that the macrocycle is located over one decyl station of the axle, the second one remaining unoccupied. In contrast, the dynamic exchange allowing the macrocycle to shuttle back and forth between the two decyl moieties is faster than the NMR timescale at high temperature (Figure S5). The ^{1}H NMR spectrum of **4a** recorded in $CDCl_2CDCl_2$

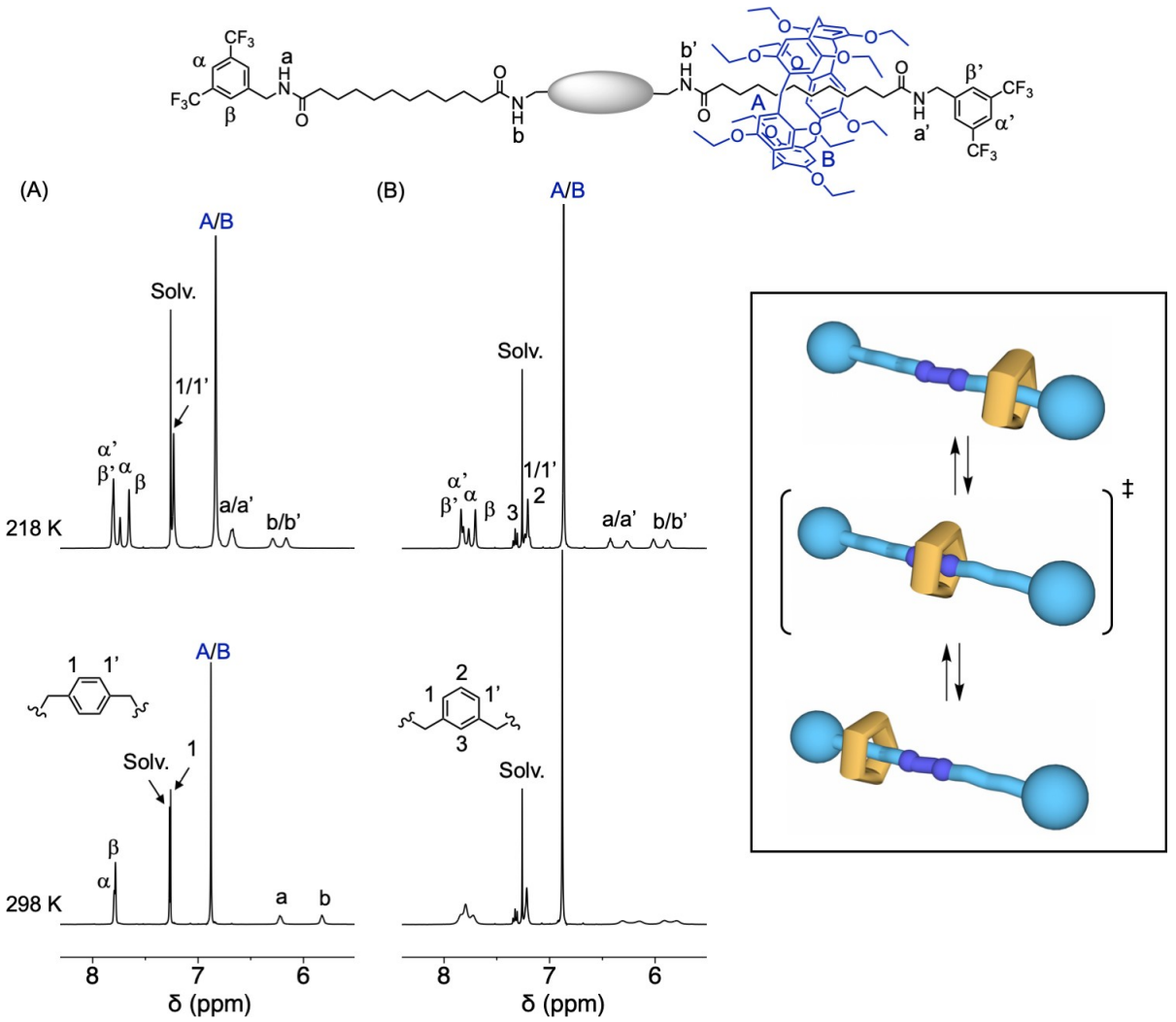

Figure 5. Aromatic region of the ^{1}H NMR spectra (400 MHz) of [2]rotaxanes **4a** (A) and **4b** (B) recorded in $CDCl_3$ at 218 and 298 K. Inset: schematic representation of the shuttling process deduced from the variable temperature ^{1}H NMR investigations, the pillar[5]arene is preferentially located over its two decyl stations in [2]rotaxanes **4a**–**d** and the central station can be considered as the transition state for the dynamic exchange allowing the macrocycle to switch from one decyl station to the other one.

revealed effectively one set of signals for the two decyl chains at 378 K. The chemical shift and the shape of the signal arising from the aromatic protons of the central *para*-phenylene moiety of **4a** are only slightly affected by the temperature changes. Indeed, the central station of **4a** is not significantly occupied by the pillar[5]arene subunit and can be considered as the transition state for the dynamic exchange. A similar behavior was observed for **4b** with the *meta*-phenylene linker. However, the gliding motions of the pillar[5]arene are slower than the NMR timescale at room temperature in this case (Figure 5). Effectively, the ^{1}H NMR spectrum of **4b** recorded at 298 K revealed non-equivalent 3,5-bis(trifluoromethyl)benzyl stoppers. By increasing the temperature, a clear coalescence was observed but the dynamic exchange was still not fast enough to obtain an average spectrum with narrow signals at the highest possible temperature that can be reached with our spectrometer (378 K). The energy barrier allowing the pillar[5]arene to shuttle back and forth between the two decyl moieties is therefore higher in the case of **4b** when compared to **4a**. Obviously, the *meta*-phenylene spacer in **4b** is more sterically demanding when compared to the *para*-phenylene linker in its isomer **4a** and crossing the central part of the axle becomes more difficult for the pillar[5]arene moiety. Variable temperature NMR investigations were also carried out for **4c** and **4d** (Figures S4 and S5). As discussed for compound **4a**, dynamic gliding motions of the macrocyclic moiety along the molecular axle of **4c** and **4d** is faster than the NMR timescale at 298 K. The two 3,5-bis(trifluoromethyl)benzamide terminated decyl chains appear effectively as equivalent under these conditions. By lowering the temperature, the dynamic gliding motions became slower than the NMR timescale for both **4c** and **4d**. As observed for **4a**, two 3,5-bis(trifluoromethyl)benzamide terminated decyl chains appeared effectively as non-equivalent in the ^{1}H NMR spectra recorded at low temperatures. In both cases, the macrocycle is located over one decyl

chain of the axle and the central station is not significantly occupied.

Overall, variable temperature ^{1}H NMR investigations revealed that the pillar[5]arene is preferentially located over its two decyl stations in [2]rotaxanes **4a–d**. In contrast, the conformer in which the macrocyclic subunit of **4a–d** is located over the central moiety of the axle is not significantly populated. Indeed, this central station can be considered as the transition state for the dynamic exchange allowing the macrocycle to shuttle back and forth between the two different decyl stations (inset Figure 5). The coalescence temperatures were found significantly different indicating changes in the activation free energy ($\Delta G^{\neq}$) of the shuttling process with the nature of the central linkers in **4a–d**. At the coalescence temperature (T_c), the rate constant (k) of the dynamic exchange is related to the chemical shift difference ($\Delta\nu$) for the two exchanging peaks bellow T_c at slow exchange regime (Eq. 1):

$$k = \frac{\pi\Delta\nu}{\sqrt{2}} \quad (1)$$

The free energy of activation ($\Delta G^{\neq}$) for the dynamic exchange can be then directly evaluated with the Eyring equation (Eq. 2):

$$\Delta G^{\neq} = -R\,T_c\,\ln(k\,h\,/\,k_B\,T_c) \quad (2)$$

where R is the gas constant, h is Planck's constant, k_B is the Boltzmann constant, T_c is the coalescence temperature, and k is the rate constant of exchange (s^{-1}). The $\Delta G^{\neq}$ values derived from the coalescence of the signals arising from the H(α) proton of the 3,5-bis(trifluoromethyl)benzyl stoppers are reported in Table 2.

The $\Delta G^{\neq}$ values were also conveniently derived from variable temperature ^{19}F NMR studies (Figure S6). As a typical example, selected ^{19}F NMR spectra recorded for **4a** are shown in Figure 6. At room temperature, only one singlet is observed. The CF_3 groups of both stoppers appear as equivalent as the shuttling of the macrocycle between its two decyl stations is faster than the NMR timescale. In contrast, by lowering the temperature, the two stoppers are not anymore equivalent and two singlets are observed. A similar behavior was also observed for **4b–d**. The $\Delta G^{\neq}$ values obtained by analyzing the coalescence of the ^{19}F NMR signals of **4a–d** are similar to the ones derived from the analysis of the ^{1}H NMR data (Table 3). In this case, the Eyring equation was also used to decompose the activation energies into enthalpic and entropic terms based on the rates of exchange deduced from the line width at $T > Tc$ according to the method described by A. M. Brouwer (Figure 6).[19] Interestingly, the activation entropy values are negative. Similar observations have been already reported for shuttling motions in rotaxanes.[19–21] Indeed, distortion of the molecular components of the rotaxanes is necessary to reach the transition state allowing the macrocycle to escape a favorable station in order to populate another one during its random walk.[21] In other words, the conformational changes required to constrain the structure are seen by the system as an ordering. On the other hand, reorganization of the solvent molecules during the shuttling process may also contribute to the negative activation entropy.

Table 2. Coalescence temperature (T_c), rate constant (k), chemical shift difference ($\Delta\nu$) and activation free energy ($\Delta G^{\neq}$) deduced from the ^{1}H NMR spectra recorded at different temperatures for [2]rotaxanes **4-d**.

[2]rotaxane	T_c (K)	$\Delta\nu$ (Hz)	k (s^{-1})	$\Delta G^{\neq}$ (kJ mol^{-1})
4a[a]	243	29.4	65.3	51(1)
4b[b]	323	28.5	63.2	68(1)
4c[c]	233	31.3	69.4	48(1)
4d[a]	233	22.3	49.5	49(1)

[a] From ^{1}H NMR spectra recorded in $CDCl_3$. [b] From ^{1}H NMR spectra recorded in $CDCl_2CDCl_2$. [c] From ^{1}H NMR spectra recorded in CD_2Cl_2.

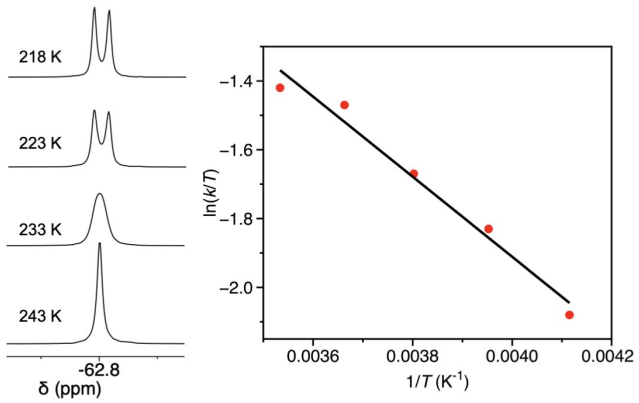

Figure 6. ^{19}F NMR spectra (376 MHz) of [2]rotaxanes **4a** recorded in $CDCl_3$ at different temperatures and the Eyring plot obtained from the rates of exchange deduced from the line width of the singlet at $T > T_c$; the $\Delta H^{\neq}$ and $\Delta S^{\neq}$ values were obtained from the slope and intercept of the plot, respectively.

Table 3. Coalescence temperature (T_c), rate constant (k), chemical shift difference ($\Delta\nu$), activation free energy ($\Delta G^{\neq}$), enthalpy of activation ($\Delta H^{\neq}$) and entropy of activation ($\Delta S^{\neq}$) deduced from the ^{19}F NMR spectra recorded in $CDCl_3$ at different temperatures for [2]rotaxanes **4a–d**.

[2]rotaxane	T_c (K)	$\Delta\nu$ (Hz)	k (s^{-1})	$\Delta G^{\neq}$ (kJ mol^{-1})	$\Delta H^{\neq}$ (kJ mol^{-1})	$\Delta S^{\neq}$ (J mol^{-1} K^{-1})
4a	233	9.2	20.4	51(1)	10(1)	−175(5)
4b	293	15.7	34.8	63(1)	19(1)	−150(5)
4c	233	10.0	22.3	51(1)	8(1)	−182(5)
4d	233	9.0	20.1	51(1)	7(1)	−185(5)

The energy barrier for the shuttling of the pillar[5]arene moiety over the central linker in **4a–d** results from an interplay between electronic and steric effects. In the case of **4c** and **4d**, steric effects are likely limited and unfavorable interactions between the triethylene glycol spacer[17] and the pillar[5]arene subunit are most probably at the origin of the energy barrier for the shuttling of the macrocycle between its two decyl stations. In the case of **4a–b**, the cavity of the pillar[5]arene is slightly too small to accommodate the central phenylene linker despite possible favorable van der Waals interactions. Effectively, the cavity size of the pillar[5]arene[22] is *ca.* 4.7 Å and the size of a phenyl ring calculated by van der Waals radii[23] *ca.* 5.0 to 5.8 Å. Obviously, substantial distortion of the pillar[5]arene scaffold is necessary to allow the phenyl group to pass through the cavity of the macrocycle. As a result, steric effects may play a major role for the shuttling of the macrocycle between the two decyl stations in the case of **4a–b**.

Density functional theory (DFT) calculations

To fully understand the preference of the pillar[5]arene for the decyl station in **4a–d**, density functional theory (DFT) calculations were carried out with appropriate fragments. Specifically, the structure of the host-guest complexes resulting from the association of methoxypillar[5]arene (**H**) with *n*-decane (**G1**), diethylene glycol dimethyl ether (**G2**) and phenylene-based model guests **G3-4** were optimized at the B3LYP/6-31G* level of theory[24] both in the gas phase and using the conductor-like polarizable continuum model (CPCM)[25] with the dielectric constant of THF (7.43) (Figure 7).

Comparison of the macrocyclic host in the B3LYP minimized structures of (**H.G1**) and (**H.G2**) with host **H** optimized at the same level revealed only limited deformations (Figure S7). The distortion energies (E_{Dist}) were then evaluated for both (**H.G1**) and (**H.G2**) by using the interaction energy decomposition method.[26] This analysis decomposes the electronic energy of the host-guest complexes into two terms, namely the distortion energy (E_{Dist}) and the interaction energy (E_{Int}). The first one corresponds to the energy required for the deformation of the individual components to form the supramolecular ensemble and the second to the difference between the electronic energies of the two distorted moieties and the host-guest complex. The overall energy gain for the complexation of each guest with **H** was then derived by adding the positive distortion energy to the negative interaction energy. The computed values are summarized in Table 4. The distortion energies are rather weak. Solvation effects are also quite limited on the distortion energies of (**H.G1**) and (**H.G2**). The interaction energies were actually not considered at the B3LYP level as dispersive interactions between molecules are not well described with this functional.[27] For this reason, the structures of (**H.G1**) and (**H.G2**) were further optimized at the ωB97X–D/6-31G* level in THF as the ωB97X–D functional includes empirical corrections for long-range dispersive interactions.[28]

The computed E_{Int} value is 15.8 kJ mol^{-1} more favorable for **G1** when compared to **G2**. As the inspection of the frontier molecular orbitals (FMOs) of (**H.G1**) and (**H.G2**) revealed the absence of electronic interactions between **H** and **G1-2** (Figure S8), the intercomponent interactions are thus purely dispersive in both cases. The difference in their E_{Int} values therefore reflects more favorable van der Waals interactions between **G1** and the pillar[5]arene receptor. Indeed, the preferential position of the pillar[5]arene over the decyl stations of **4c** and **4d** results from stronger dispersive interactions between the pillar[5]arene and the peripheral decyl stations when compared to the central triethylene glycol station. On the other hand, differences in solvation between the two stations may also play a role. To further elucidate the factors governing the random walk of the pillar[5]arene moiety in rotaxanes **4c**

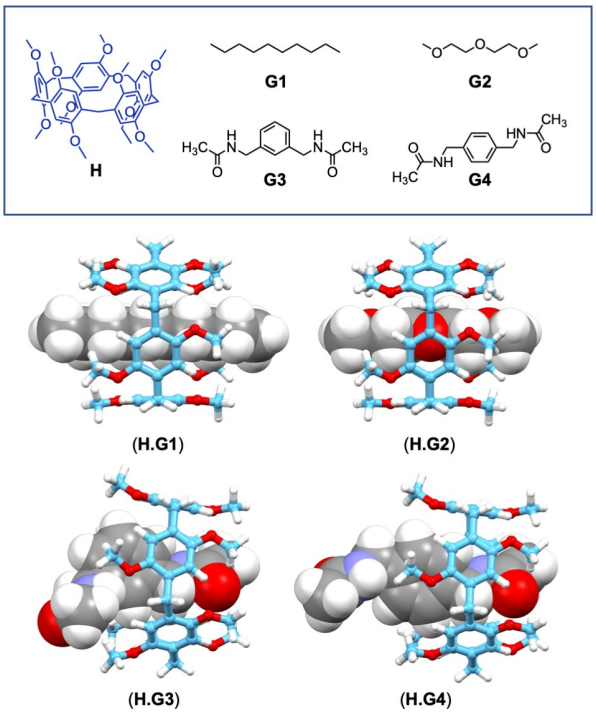

Figure 7. Fragments used for the DFT calculations and structures of (**H.G1-4**) optimized in the gas phase at the B3LYP/6-31G* level (H: white, O: red, N: blue, C: grey for **G1-4** and pale blue for **H**).

Table 4. Distortion and interaction energies calculated for (**H.G1**) and (**H.G2**).

Host-guest complex	E_{Dist} (kJ mol^{-1})	E_{Int} (kJ mol^{-1})	$E_{Dist} + E_{Int}$ (kJ mol^{-1})
B3LYP/6-31G* (gas phase)			
(**H.G1**)	4.2		
(**H.G2**)	8.0		
B3LYP/6-31G* (THF)			
(**H.G1**)	4.5		
(**H.G2**)	5.0		
ωB97X–D/6-31G* (THF)			
(**H.G1**)	9.7	−175.3	−165.6
(**H.G2**)	7.3	−159.5	−152.2

and **4d**, the slipping of **G1** and **G2** through macrocyclic host **H** was computed in a stepwise manner (Figure S9). The resulting structures were then subjected to a distortion/interaction analysis (Figure 8).

In the case of (**H.G1**), the distortion energy remains almost constant whatever the position of **H** over the *n*-decane chain. The variations of the interaction energies are ascribed to the different relative orientations of **H** and **G1** modulating the strength of intercomponent C–H···π interactions in (**H.G1**). Gliding motions of the pillar[5]arene along the decyl station in **4a-d** can therefore be seen in successive small random jumps from one local minimum to a neighboring one with a very low energy barrier to overcome. The system is in a way continuously searching to counterbalance the thermal agitation by optimizing the weak intercomponent C–H···π interactions between the methylene groups of the axle and the pillar[5]arene moiety. In other words, the motions of the pillar[5]arene over their decyl station are Brownian motions consisting in random fluctuations.

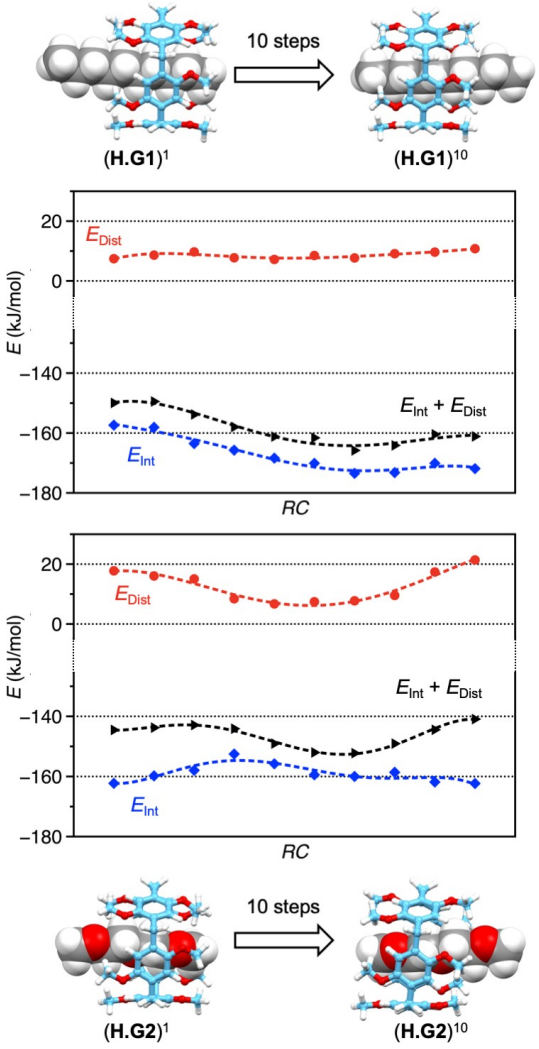

Figure 8. Distortion/interaction analysis of the structures obtained from the energy profile calculated for the slipping of guest **G1** (top) and **G2** (bottom) through macrocyclic host **H** (ωB97X–D/6-31G* level using the CPCM model with the dielectric constant of THF; H: white, O: red; C: grey for **G1-2** and pale blue for **H**).

For (**H.G2**), substantial variations of distortion energy are observed when the pillar[5]arene moiety slides over the ethylene glycol chain (Figure 8). The distortion energy is increased as soon as an oxygen atom of **G2** is located close to the five O atoms of one rim of **H**. Actually, repulsive interactions between the oxygen atoms are at the origin of a slight tilt of the hydroquinone subunits of **H**. The most favorable situation in terms of interaction and distortion energies is observed when the central O atom of **G2** is located in the middle of the cavity of **H**. In this conformation, methylene subunits of **G2** are located close to the O atoms of **H** thus preventing the distortion of the macrocyclic receptor. At the same time, favorable intercomponent C–H···π interactions take place between two hydroquinone moieties of **H** and the two central CH_2 groups of **G2**. Overall, the observed energy barrier for the shuttling of the macrocycle in **4c-d** accounts in part for the energy necessary to overcome the enthalpic and solvation changes when going from a decyl station to the triethylene glycol one. However, steric effects play also a significant role as distortion of the macrocycle occurs when the O atoms of both the triethylene glycol station and the pillar[5]arene are close to each other. This substantial steric constrain highlighted by the DFT calculations is also consistent with the negative activation entropy deduced experimentally from the variable temperature NMR studies.

Similar DFT calculations were also carried out with the host-guest complexes resulting from the association of **H** with phenylene-based model guests **G3-4**. As shown in Figure 7, the pillar[5]arene host has to tilt one of its hydroquinone unit to accommodate guests **G3** and **G4** within its cavity. Nonetheless, in both cases, the phenylene moiety is not located within the cavity of the host thus confirming that the pillar[5]arene cavity is slightly too small to host a 6-membered aromatic ring. Energy profiles were also calculated for (**H.G3**) and (**H.G4**) to visualize how the pillar[5]arene moiety slides over the phenylene stations in [2]rotaxanes **4a** and **4b** (Figure S10). The energy profile together with selected calculated structures are shown in Figure 9. In the case of (**H.G4**), the energy gradually increases as the phenylene moiety of **G4** begins to pass through the cavity of **H**. Near the transition state, the entire cyclophane scaffold of **H** bends slightly and the tilted hydroquinone subunit of **H** then swings over the phenyl ring of **G4** thus allowing the guest to escape on the other side. As soon as the phenylene group has sufficiently crossed the median plane of the cavity, the applied distance constraint is reoriented by the system. As a result, the orientation of the guest relative to the host is modified thus leading to a non-continuous profile. The calculations done with host **G3** show the same qualitative trends (Figure 9). Steric constraints are however more important due to the *meta*-substitution pattern of the phenylene moiety of **G3**. Indeed, the aromatic subunit of **G3** is forced to cross the cavity with two *para*-CH groups parallel to the plane of the cavity of the pillar[5]arene. As a result, the width of the phenylene is greater than in the case of the *para* analogue (**G3**) which can cross the cavity with a more favorable orientation. In the particular case of **G3**, the energy profile shows an abrupt drop after the transition state. Indeed, as soon as the phenylene group has sufficiently crossed the median plane of the cavity, the system

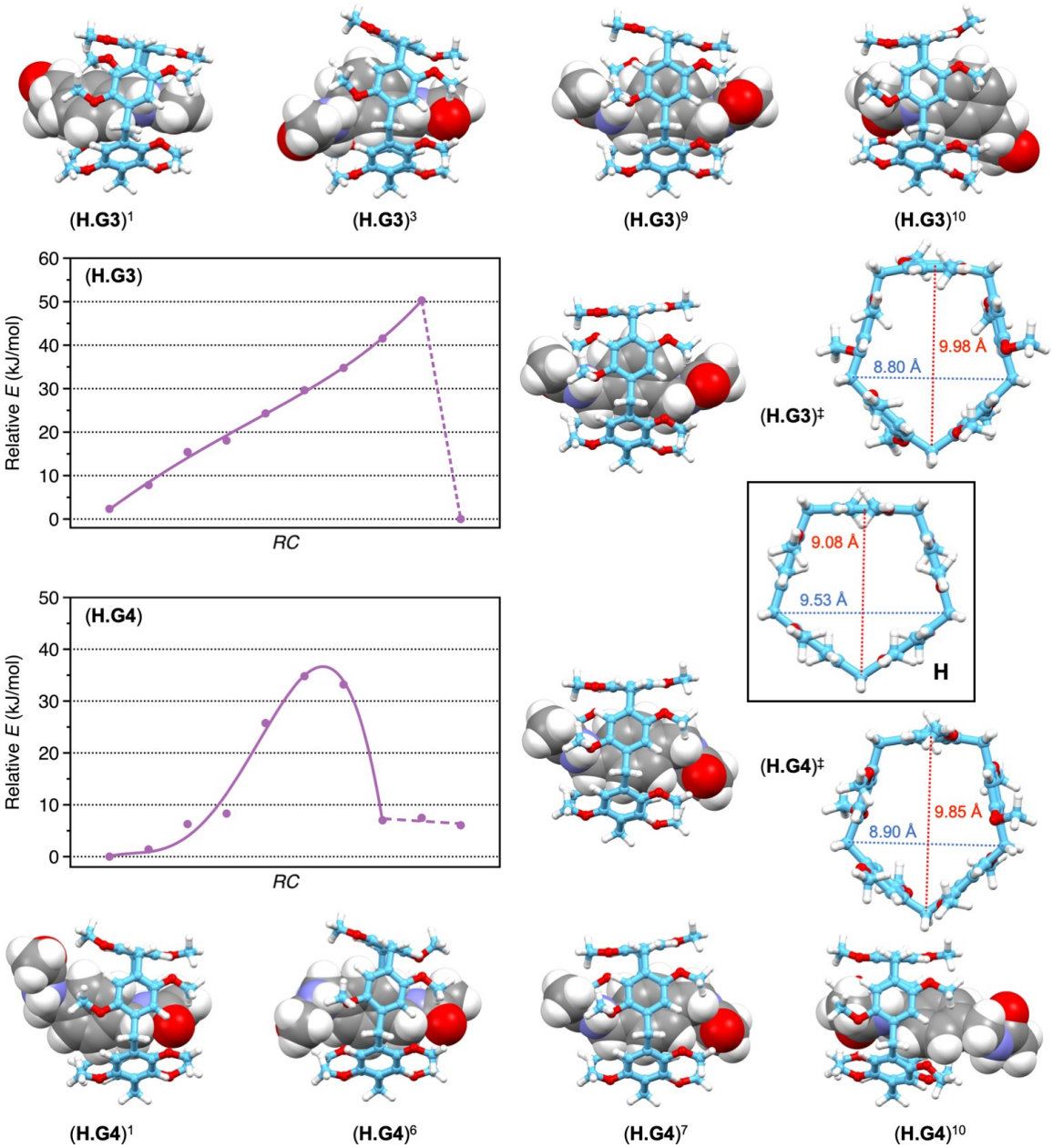

Figure 9. Selected structures of (**H.G3**) and (**H.G4**) obtained from the energy profile calculated for the slipping of guest **G3** (top) and **G4** (bottom) through macrocyclic host **H**. The transition states (**H.G3**)‡ and (**H.G4**)‡ found for the slippage process are also shown together with a comparison of the **H** moiety of (**H.G3**)‡ and (**H.G4**)‡ with the structure of **H** (inset). All the represented structures have been optimized in the gas phase at the B3LYP/6-31G* level (H: white, O: red, N: blue, C: grey for **G1-4** and pale blue for **H**).

directs the distance constraint towards the outside of the cavity and no longer towards the inside.

In both cases, transition states were also computed (Figure 9). As revealed by the frequency analysis, just one imaginary frequency was associated with each transition state. Visual inspection of the corresponding normal mode validated also the identification of the transition states. Close analysis of (**H.G3**)‡ and (**H.G4**)‡ shows a large deformation of the cyclophane core of **H**. The pillar[5]arene is shrinking its structure in one direction to increase the height of its cavity in the perpendicular direction. In this way, the cavity is able to accommodate the phenylene moiety of the guest. When compared to the optimized structure of **H** for which the height is 9.08 Å, an increase of 0.90 and 0.77 Å is observed in the transition states (**H.G3**)‡ and (**H.G4**)‡, respectively. Clearly, the distortion of the pillar[5]arene is more important in the case of (**H.G3**)‡. The structural factors controlling the slippage of the pillar[5]arene over the phenylene moieties of **G3** and **G4** were further investigated by evaluating the energy required for the deformation of their individual components (**H** and **G3-4**) in transition states (**H.G3**)‡ and (**H.G4**)‡. The distortion energies are summarized in Table 5.

As expected from the difference in free energy of activation experimentally determined by analyzing the coalescence of the

Table 5. Distortion and interaction energies calculated for transition states $(\mathbf{H.G3})^{\ddagger}$ and $(\mathbf{H.G4})^{\ddagger}$.

Transition state	E_{Dist} (kJ mol^{-1})	E_{Int} (kJ mol^{-1})	$E_{Dist} + E_{Int}$ (kJ mol^{-1})
B3LYP/6-31G* (gas phase)			
$(\mathbf{H.G3})^{\ddagger}$	55.1		
$(\mathbf{H.G4})^{\ddagger}$	46.6		
ωB97X–D/6-31G* (THF)			
$(\mathbf{H.G3})^{\ddagger}$	58.9	−199.4	−140.5
$(\mathbf{H.G4})^{\ddagger}$	53.2	−199.7	−146.5

NMR signals of **4a** and **4b**, the distortion energies computed for the *para*- and *meta*-phenylene-containing model transition states $(\mathbf{H.G4})^{\ddagger}$ and $(\mathbf{H.G3})^{\ddagger}$ are quite high. Whereas the binding of **G1** is governed by dispersive interactions, the situation is totally different for **G3-4**. In both cases, favorable electronic interactions are effectively evidenced by a stabilization of the highest occupied HOMO of **H** and a destabilization of the lowest unoccupied molecular orbital (LUMO) of **G3-4** in the host-guest complexes calculated with the phenylene groups located within the cavity of the pillar[5]arene (Figure S11). This is reflected by the significantly larger E_{Int} values obtained for $(\mathbf{H.G3})^{\ddagger}$ and $(\mathbf{H.G4})^{\ddagger}$, when compared to those calculated for (**H.G1**) (Tables 4 and 5). However, these more favorable interaction energies are counterbalanced by the high distortion energies. As a result, the overall energy gain for the complexation of **G3-4** is largely penalized by the high distortion energy and steric factors explains the more favorable formation of (**H.G1**). In the case of rotaxanes **4a–b**, the limited distortion of the macrocyclic component is therefore at the origin of the preferential location of the pillar[5]arene moiety over the decyl stations. Moreover, the DFT calculations revealed also that the shuttling of the macrocycle between the two decyl stations in **4a–b** is essentially governed by steric effects.

Computational studies were also carried out in order to evaluate the distance over which the gliding motions of the pillar[5]arene moiety are possible in the case of [2]rotaxanes **4a–d**. Geometry optimizations were performed at the semi-empirical level (PM6). The calculated structures are shown in Figure 10. The length of the decyl stations of the rotaxanes is *ca.* 1.39 nm. The width of the pillar[5]arene moiety is *ca.* 1 nm if one considers its ethoxy substituents. Gliding motions of the pillar[5]arene component over its axle subunit occurs over a distance of *ca.* 3.8–4.2 nm depending on the nature of the central spacer. Despite the relatively large length of the axle, the dynamic exchange allowing the macrocycle to shuttle back and forth between the two different decyl stations remains faster than the NMR timescale at room temperature in the case of **4a** and **4c–d**. In the particular case of **4b**, higher temperature are necessary to allow motions of the pillar[5]arene over the entire length of the axle due to a greater energy barrier to cross the substantially larger central subunit.

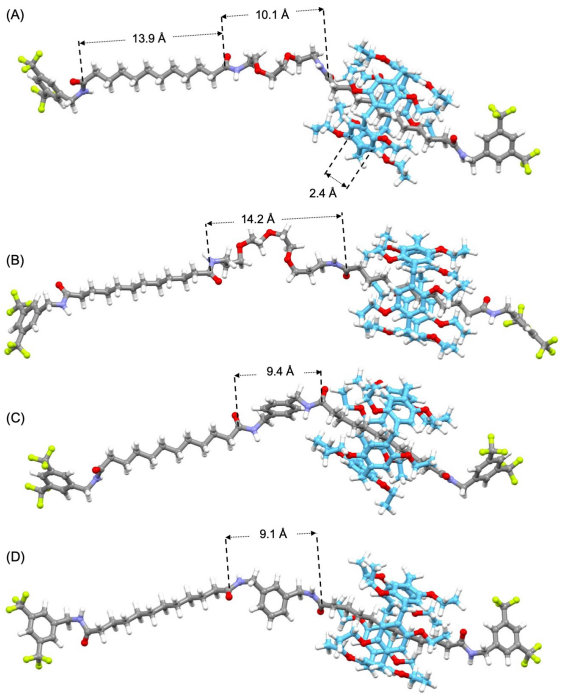

Figure 10. Calculated structures of compounds **4c** (A), **4d** (B), **4a** (C) and **4b** (D) highlighting the distances between the C atoms of the C=O moieties of the axle component and the C–C distance between two aromatic C atoms of the pillar[5]arene moiety (H: white, F: light green, O: red, N: blue, C: grey for the axle and pale blue for the pillar[5]arene moiety).

Conclusions

In this paper, the reaction between a rotaxane building block bearing an activated pentafluorophenyl ester stopper and various diamine reagents has been investigated. When the diamine reagent is large enough to prevent dissociation of the monoacylated intermediate, reaction with a second equivalent of the rotaxane building block provides the corresponding [3]rotaxane in excellent yields. In contrast, when the diamine reagent is smaller, the monoacylated intermediate is an inclusion complex. In THF solutions, complete dissociation of the inclusion complex occurred. As a result, the amine function of the resulting molecular thread with the pentafluorophenyl ester stoppered rotaxane affords the corresponding [2]rotaxane with an elongated axle unit. In contrast, when the reaction is performed under solvent-free mechanochemical conditions, dissociation of the intermediate inclusion complex is partially prevented thus allowing the formation of [3]rotaxanes. As far as the synthesis is concerned, the present work illustrates the potential of the stopper exchange strategy for the construction of sophisticated rotaxanes that would be difficult to obtain by classical synthetic strategies based on the direct introduction of stoppers onto the axle moiety of a preorganized host-guest complex. On the other hand, detailed conformational investigations have been also carried out by variable temperature NMR investigations. To fully understand the motions of the pillar[5]arene subunit along the axles of the rotaxanes reported therein, DFT calculations have been particularly useful. The

preferential location of the macrocycle over particular stations results from an interplay between favorable intercomponent interactions and deformation of the constitutive elements of the rotaxanes. Such considerations are essential for the further development of pillar[5]arene-based molecular machines in which the position of the macrocycle can be controlled by an external stimuli. Work in this direction is currently underway in our laboratory.

Experimental section

Synthesis. The characterization of all the new compounds is described in the Supporting Information. Compound **2**[14] was prepared according to a reported procedure.

General procedure for the preparation of [2]rotaxanes 4a–d and [3]rotaxane 5e in solution. A mixture of **2** (2.0 eq.) and the appropriate diamine reagent (**3a–e**, 1.0 eq.) in anhydrous THF (1 mL/110 mg of **2**) was stirred at rt for 6 days (**4a–d**) or 2 days (**5e**). The resulting mixture was filtered through a short plug (SiO_2, CH_2Cl_2 containing 5% MeOH), concentrated and purified by gel permeation chromatography (Biobeads SX-1, $CHCl_3$).

General procedure for the preparation of [2]rotaxanes 4a-c and [3]rotaxanes 5a–c under mechanochemical conditions. Compound **2** (2.2 eq.), the appropriate diamine reagent (**3a–c**, 1.0 eq.) and TBD (2.0 eq.) were placed in a stainless-steel vial containing four stainless-steel balls. The resulting mixture was mixed in a Retsch MM400 mill at 30 Hz for 2 h. The crude was filtered through a short plug (SiO_2, $CHCl_3$ containing 5% MeOH), concentrated and purified by gel permeation chromatography (Biobeads SX-1, $CHCl_3$).

Supporting Information

The authors have cited additional references within the Supporting Information.[29,30]

Acknowledgements

Financial support from the ANR (projects FastGiant ANR-17-CE07-0012-01 and Pillar ANR-19-CE06-0032), the *Fondation Jean-Marie Lehn*, the LabEx *"Chimie des Systèmes Complexes"*, and the Tunisian Ministry of Higher Education and Scientific Research and Technology is gratefully acknowledged. We also thank Dr. M. Holler for helpful discussions and C. Chervier-Legourd for the preparation of some starting materials.

Conflict of Interests

The authors declare no conflict of interest.

Data Availability Statement

The data that support the findings of this study are available in the supplementary material of this article.

Keywords: rotaxane · pillar[5]arene · stopper exchange · distortion energy · molecular shuttles

[1] a) J.-P. Sauvage, C. Dietrich-Buchecker (Eds.), *Molecular Catenanes, Rotaxanes and Knots – A Journey Through the World of Molecular Topology*, J. Wiley and Sons, **2008**; b) C. J. Bruns, J. F. Stoddart, *The Nature of the Mechanical Bond – From Molecules to Machines*, J. Wiley & Sons, **2016**.

[2] a) R. A. Bissell, E. Córdova, A. E. Kaifer, J. F. Stoddart, *Nature* **1994**, *369*, 133–137; b) A. Livoreil, C. O. Dietrich-Buchecker, J.-P. Sauvage, *J. Am. Chem. Soc.* **1994**, *116*, 9399–9400; c) J.-P. Sauvage, *Angew. Chem. Int. Ed.* **2017**, *56*, 11080–11093; *Angew. Chem.* **2017**, *129*, 11228–11242; d) J. F. Stoddart, *Angew. Chem. Int. Ed.* **2017**, *56*, 11228–11242; *Angew. Chem.* **2017**, *129*, 11244–11277.

[3] For a recent review, see: S. R. Beeren, C. T. McTernan, F. Schaufelberger, *Chem* **2023**, *9*, 1378–1412.

[4] a) Y. Feng, M. Ovalle, J. S. W. Seale, C. K. Lee, D. J. Kim, R. D. Astumian, J. F. Stoddart, *J. Am. Chem. Soc.* **2021**, *143*, 5569–5591; b) M. Baroncini, S. Silvi, A. Credi, *Chem. Rev.* **2020**, *120*, 200–268; c) S. Corra, M. Curcio, M. Baroncini, S. Silvi, A. Credi, *Adv. Mater.* **2020**, *32*, 1906064; d) H. V. Schröder, C. A. Schalley, *Chem. Sci.* **2019**, *10*, 9626–9639; e) A. Coskun, M. Banaszak, R. D. Astumian, J. F. Stoddart, B. A. Grzybowski, *Chem. Soc. Rev.* **2012**, *41*, 19–30.

[5] a) C. Kwamen, J. Niemeyer, *Chem. Eur. J.* **2021**, *27*, 175–186; b) G. Olivo, G. Capocasa, D. Del Giudice, O. Lanzalunga, S. Di Stefano, *Chem. Soc. Rev.* **2021**, *50*, 7681–7724; c) A. Martinez-Cuezva, A. Saura-Sanmartin, M. Alajarin, J. Berna, *ACS Catal.* **2020**, *10*, 7719–7733; d) V. Blanco, D. A. Leigh, V. Marcos, *Chem. Soc. Rev.* **2015**, *44*, 5341–5370; e) S. Erbas-Cakmak, D. A. Leigh, C. T. McTernan, A. L. Nussbaumer, *Chem. Rev.* **2015**, *115*, 10081–10206; f) E. A. Neal, S. M. Goldup, *Chem. Commun.* **2014**, *50*, 5128–5142.

[6] a) J. E. M. Lewis, P. D. Beer, S. J. Loeb, S. M. Goldup, *Chem. Soc. Rev.* **2017**, *46*, 2577–2591; b) N. H. Evans, P. D. Beer, *Chem. Soc. Rev.* **2014**, *43*, 4658–4683; c) G. T. Spece, P. D. Beer, *Acc. Chem. Res.* **2013**, *46*, 571–586; d) R. S. Forgan, J.-P. Sauvage, J. F. Stoddart, *Chem. Rev.* **2011**, *111*, 5434–5464; e) J. D. Crowley, S. M. Goldup, A.-L. Lee, D. A. Leigh, R. T. McBurney, *Chem. Soc. Rev.* **2009**, *38*, 1530–1541.

[7] M. A. Hood, M. Mari, *Rotaxane Synthesis and Applications Chemistry*, Intelliz Press, **2016**.

[8] For a review on pillar[5]arene-containing mechanically interlocked systems, see: K. Kato, S. Fa, S. Ohtani, T-h. Shi, A. M. Brouwer, T. Ogoshi, *Chem. Soc. Rev.* **2022**, *51*, 3648–3687.

[9] R. Milev, A. Lopez-Pacheco, I. Nierengarten, T. M. N. Trinh, M. Holler, R. Deschenaux, J.-F. Nierengarten, *Eur. J. Org. Chem.* **2015**, 479–485.

[10] a) N. L. Strutt, R. S. Forgan, J. M. Spruell, Y. Y. Botros, J. F. Stoddart, *J. Am. Chem. Soc.* **2011**, *133*, 5668–5671; b) T. Ooshi, T. Aoki, R. Shiga, R. Iisuka, S. Ueda, K. Demachi, D. Yamafuji, H. Kayama, T.-a. Yamagishi, *J. Am. Chem. Soc.* **2012**, *134*, 20322–20325; c) P. Wei, X. Yan, J. Li, Y. Ma, Y. Yao, F. Huang, *Tetrahedron* **2012**, *68*, 9179–9185; d) S. Dong, C. Han, B. Zheng, M. Zhang, F. Huang, *Tetrahedron Lett.* **2012**, *53*, 3668–3671; e) A. Mapp, J. T. Wilmore, P. D. Beer, J. M. Goicoechea, *Angew. Chem. Int. Ed.* **2023**, *62*, e202309211; *Angew. Chem.* **2023**, *135*, e202309211.

[11] a) I. Nierengarten, E. Meichsner, M. Holler, P. M. Pieper, R. Deschenaux, B. Delavaux-Nicot, J.-F. Nierengarten, *Chem. Eur. J.* **2018**, *24*, 169–177; b) I. Nierengarten, J.-F. Nierengarten, *ChemistryOpen* **2020**, *9*, 393–400; c) M. Rémy, I. Nierengarten, B. Park, M. Holler, U. Hahn, J.-F. Nierengarten, *Chem. Eur. J.* **2021**, *27*, 8492–8499.

[12] The concept of stopper exchange for the post-modification of rotaxanes has been introduced by Stoddart and co-workers, see: a) S. J. Rowan, J. F. Stoddart, *J. Am. Chem. Soc.* **2000**, *122*, 164–165; b) S. J. Rowan, S. J. Cantrill, J. F. Stoddart, A. J. P. White, D. J. Williams, *Org. Lett.* **2000**, *2*, 759–762.

[13] The post-modification of pre-constructed [2]rotaxanes by stopper exchange reactions has been rarely used and only a few examples have been reported so far, see: a) R. J. Bordoli, S. M. Goldup, *J. Am. Chem. Soc.* **2014**, *136*, 4817–4820; b) D. W. Zehnder II, D. B. Smithrud, *Org. Lett.* **2001**, *3*, 2485–2487; c) N. Kihara, S. Motoda, T. Yokozawa, T. Takata, *Org. Lett.* **2005**, *7*, 1199–1202; d) J. S. Hannam, S. M. Lacy, D. A. Leigh, C. G. Saiz, A. M. Z. Slawin, S. G. Stitchell, *Angew. Chem. Int. Ed.* **2004**, *43*, 3260–3264; e) S. C. Rajappan, D. R. McCarthy, J. P. Campbell, J. B. Ferrel, M. Sharafi, O. Ambrozaite, J. Li, S. T. Schneebeli, *Angew. Chem. Int. Ed.* **2020**, *59*, 16668–16674.

[14] N. Becharguia, E. Wasielewski, R. Abidi, I. Nierengarten, J.-F. Nierengarten, *Chem. Eur. J.* **2023**, e202303501 (in press).

[15] a) A. Orita, J. Okano, Y. Tawa, L. Jiang, J. Otera, *Angew. Chem. Int. Ed.* **2004**, *43*, 3724–3728; b) S. Y. Hsueh, K. W. Cheng, C.-C. Lai, S.-H. Chiu, *Angew. Chem. Int. Ed.* **2008**, *47*, 4436–4439; c) C.-C. Hsu, N. C. Chen, C.-C. Lai, Y.-H. Liu, S.-M. Peng, S.-H. Shiu, *Angew. Chem. Int. Ed.* **2008**, *47*, 7475–7478; d) C.-C. Hsu, C.-C. Lai, S.-H. Chiu, *Tetrahedron* **2009**, *65*, 2824–2829; e) P.-N. Chen, C.-C. Lai, S.-H. Chiu, *Org. Lett.* **2011**, *13*, 4660–4663; f) K.-D. Wu, Y.-H. Lin, C.-C. Lai, S.-H. Chiu, *Org. Lett.* **2014**, *16*, 1068–1071; g) H.-G. Li, G.-W. Wang, *J. Org. Chem.* **2017**, *82*, 6341–6348; h) K. Wada, K. Yasuzawa, S. Fa, Y. Nagata, K. Kato, S. Ohtani, T. Ogoshi, *J. Am. Chem. Soc.* **2023**, *145*, 15324–15330; i) for a review on supramolecular concepts in mechanochemistry, see: T. Friščić, *Chem. Soc. Rev.* **2012**, *41*, 3493–3510.
[16] M. Holler, T. Stoerkler, A. Louis, F. Fisher, J.-F. Nierengarten, *Eur. J. Org. Chem.* **2019**, 3401–3405.
[17] T.-w. Kwon, B. Song, K. W. Nam, J. F. Stoddart, *J. Am. Chem. Soc.* **2022**, *144*, 12595–12601.
[18] I. Nierengarten, K. Buffet, M. Holler, S. P. Vincent, J.-F. Nierengarten, *Tetrahedron Lett.* **2013**, *54*, 2398–2402.
[19] D. D. Günbas, A. M. Brouwer, *J. Org. Chem.* **2012**, *77*, 5724–5735.
[20] a) S. Garaudé, S. Silvi, M. Venturi, A. Credi, A. H. Flood, J. F. Stoddart, *ChemPhysChem* **2005**, *6*, 2145–215; b) D. C. Jagesar, S. M. Fazio, J. Taybi, E. Eiser, F. G. Gatti, D. A. Leigh, A. M. Brouwer, *Adv. Funct. Mater.* **2009**, *19*, 3440–3449.
[21] M. R. Panman, P. Bodis, D. J. Shaw, B. H. Bakker, A. C. Newton, E. R. Kay, A. M. Brouwer, W. J. Buma, D. A. Leigh, S. Woutersen, *Science* **2010**, *328*, 1255–1258.
[22] T. Ogoshi, T.-a. Yamagishi, Y. Nakamoto, *Chem. Rev.* **2016**, *116*, 7937–8002.
[23] a) X. Zhang, F. Rösicke, V. Syritski, G. Sun, J. Reur, K. Hinrichs, S. Janietz, J. Rappich, *Z. Phys. Chem.* **2014**, *228*, 557–573; b) A. Bondi, *J. Phys. Chem.* **1964**, *68*, 441–451.
[24] A. D. Becke, *J. Chem. Phys.* **1993**, *98*, 5648–5652.
[25] a) T. N. Truong, E. V. Stefanovich, *Chem. Phys. Lett.* **1995**, *240*, 253–260; b) V. Barone, M. Cossi, *J. Phys. Chem. A* **1998**, *102*, 1995–2001.
[26] a) S. V. Athare, S. P. Gejji, *J. Phys. Chem. A* **2019**, *123*, 8391–8396; b) M. Panneerselvam, M. D. Kumar, M. Jaccob, R. V. Solomon, *ChemistrySelect* **2018**, *3*, 1321–1334; c) J.-F. Nierengarten, *J. Porphyrins Phthalocyanines* **2023**, *27*, 1253–1262.
[27] E. F. Grossman, D. A. Daramola, G. G. Botte, *ChemOpen* **2021**, *10*, 316–326.
[28] J.-D. Chai, M. Head-Gordon, *J. Chem. Phys.* **2008**, *128*, 084106.
[29] I. Nierengarten, M. Nothisen, D. Sigwalt, T. Biellmann, M. Holler, J.-S. Remy, J.-F. Nierengarten, *Chem. Eur. J.* **2013**, *19*, 17552–17558.
[30] Y. Shao, L. F. Molnar, Y. Jung, J. Kussmann, C. Ochsenfeld, S. T. Brown, A. T. B. Gilbert, L. V. Slipchenko, S. V. Levchenko, D. P. O'Neill, R. A. D. Jr, R. C. Lochan, T. Wang, G. J. O. Beran, N. A. Besley, J. M. Herbert, C. Y. Lin, T. V. Voorhis, S. H. Chien, A. Sodt, R. P. Steele, V. A. Rassolov, P. E. Maslen, P. P. Korambath, R. D. Adamson, B. Austin, J. Baker, E. F. C. Byrd, H. Dachsel, R. J. Doerksen, A. Dreuw, B. D. Dunietz, A. D. Dutoi, T. R. Furlani, S. R. Gwaltney, A. Heyden, S. Hirata, C.-P. Hsu, G. Kedziora, R. Z. Khalliulin, P. Klunzinger, A. M. Lee, M. S. Lee, W. Liang, I. Lotan, N. Nair, B. Peters, E. I. Proynov, P. A. Pieniazek, Y. M. Rhee, J. Ritchie, E. Rosta, C. D. Sherrill, A. C. Simmonett, J. E. Subotnik, H. L. W. III, W. Zhang, A. T. Bell, A. K. Chakraborty, D. M. Chipman, F. J. Keil, A. Warshel, W. J. Hehre, H. F. S. III, J. Kong, A. I. Krylov, P. M. W. Gill, M. Head-Gordon, *Phys. Chem. Chem. Phys.* **2006**, *8*, 3172–3191.

Manuscript received: December 11, 2023
Accepted manuscript online: January 2, 2024
Version of record online: January 2, 2024

RESEARCH ARTICLE

Stopper exchange reactions between a rotaxane building block and diamine reagents gave dramatically different outcome in solution and in solvent-free conditions. Upon a first acylation, an intermediate host-guest complex with a terminal amine function is obtained. Dissociation of the intermediate occurs in solution but the inclusion complex is preserved under mechanochemical solvent-free conditions.

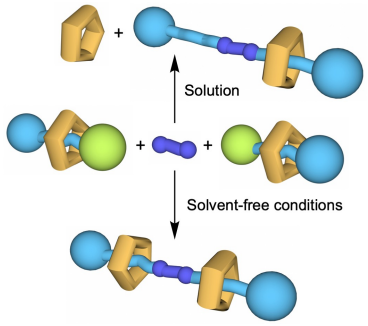

Dr. N. Becharguia, Dr. I. Nierengarten, Dr. J.-M. Strub, Dr. S. Cianférani, Dr. M. Rémy, Dr. E. Wasielewski, Prof. R. Abidi, Dr. J.-F. Nierengarten**